EPJ Web of Conferences **94**, 05001 (2015)
DOI: 10.1051/epjconf/20159405001

Industrial application of Instrumented DWTT in evaluating material resistance to ductile fracture for modern pipeline steels

Jian Fang[1,a], Jian-wei Zhang[1], and Xing Huang[2]

[1] Baosteel Research Institute, Baoshan Iron & Steel Co., Ltd., Shanghai 201900, China
[2] Shenzhen WANCE Testing Machine Co., Ltd., Shenzhen 518055, China

Abstract. $CTOA_C$ of typical X70, X80 and X90 pipeline steels plates were evaluated by using energy based regression method upon their single specimen. Clear difference in the material resistance to ductile cracking could be distinguished by the values of $CTOA_C$ and their characteristic fracture surface. The region of stable cracking on the fracture surface could be identified from the dynamic crack extension curve, with the help of key-curve method. In the meanwhile, the crucial material based parameter required by many other $CTOA_C$ algorithm, $(A^*\sigma_f)$ of present X70, X80 and X90 plates were experimentally determined, also proving the validity of theoretical geometric factor A^* to be 0.30–0.34, close to the commonly cited constant of 1/3.

1. Introduction

Drop-Weight-Tear-Test (DWTT) has been widely applied as an alternative mill trial to characterize the material resistance to ductile facture for modern high strength and toughness pipeline steels, like X70, X80. Considering the larger ligament of DWTT specimen for crack propagating, the results from DWTT including fracture appearance, Ductile Brittle Transition Temperature value are usually consistent with the full-scale tests, more than Charpy test using sub-size specimens. Most significantly, the critical Crack Tip Opening Angle, $CTOA_C$ over the steady-state stage of crack propagation derived from DWTT [1] has been also ascertained as a measure of crack arrest capacity, conveniently and economically conducted in a mill test. In the recent works, a single-specimen energy based regression method [2] to estimate $CTOA_C$ has been proposed on the basis of well-known Martinelli-Venzi rigid-plastic ductile fracture model [3]. By using the regression of absorbed energy against the impact load as input, the regression method shall give more reliable consequences than conventional simple energy input approaches [4]. However, how to define the regression range especially confined in the steady-state stage is still a technical difficulty and influence the quality of $CTOA_C$ results.

In the present study, key-curve method [5] has been introduced to link the microscopic ductile cracking behaviour from the obtained DWTT force-displacement curve to the captured macroscopic fracture surface of broken DWTT specimen, helpful to the accurate definition of stable region for ductile fracture.

2. Principles

2.1. Energy based regression method

As above, V-notch pressed DWTT specimens are commonly used for a mill test. The single-specimen energy based regression method for a DWTT-type specimen is described as Eq. (1).

$$CTOA_C = 2\arctan\left[\frac{-4r^*}{S}\cdot\frac{\Delta E}{\Delta P}\right]_{a_1\to a_2}. \quad (1)$$

Where, S is the span between two support rollers (= 254 mm), r^* is a rotation factor, for DWTT specimens with larger ligaments, it has been determined to be 0.57 for high-strength steels including API X70–X100 pipeline steel appropriately [6].

Thus, the regression value of impact energy vs. load within the stable cracking range that is defined by the crack length from a_1 to a_2 may be used to evaluate instantaneous $CTOA_C$, only requiring values of r^* and S.

2.2. Key-curve method

Key-curve (KC) method developed by Kobayashi [5] has been proved satisfactorily to estimate the dynamic crack extension based on the instrumented impact. The procedure of KC method is described in Eqs. (2) and (3). (more detailed in Ref. [2]) Firstly, the key curve is analytically established by fitting the original relationship between the force (P) and displacement (y) on the pre-peak part of the instrument curve, obtaining the parameters k and n.

$$\frac{PW}{b_0^2} = k\left(\frac{y}{W}\right)^n. \quad (2)$$

Where, P is impact load, b_0 (= W − a_0) is the initial ligament width, y is load line displacement by the tup as

[a] Corresponding author: fangjian@baosteel.com

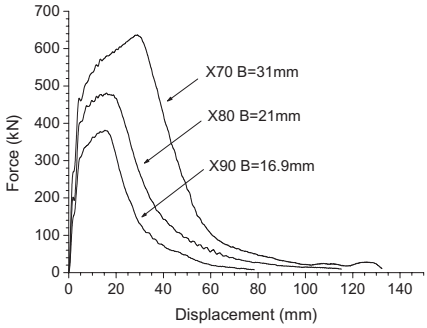

Figure 1. Curves for different instrumented DWTT samples.

above. n and k are material based constants, which should be determined on each force-displacement relationship by curve fitting from the beginning to the maximum force point.

Secondly, an amount of the crack extension could be estimated at any displacement on the post-peak part of the load-displacement curve, as Eq. (2).

$$\Delta a = W - \left(\left(\frac{P W^{n+1}}{k y^n} \right)^{1/2} + a_0 \right) \cdot \qquad (3)$$

As a result, an amount of the crack extension is to be estimated at any displacement on the post-peak part of force-displacement curve.

3. Experimental

An instrumented pendulum impact machine with 40 kJ capacity and 8 m/s velocity was used to apply DWTT tests at room temperature on the standard V-notch pressed specimens sampled from three typical API X70, X80 and X90 pipeline steel plates. Given the machine's physical parameters like hammer mass, velocity, etc., the instrument load-displacement relation could be calculated by double integration of recorded load-time trace from the force measuring device (including the instrumented tup and AD/DA units), based on the Newton's law. Consequently, the total DWTT energy could be subdivided into the crack initiation and propagation parts, as illustrated in Fig. 1.

After preparation of the instrumented tup and being statically calibrated linearly over the load scale up to 800kN (accuracy better than ±1%, relative error), the DWTT energy calculated by instrument method is nearly the same as the measured from the pendulum dial, less than ±2% (full measurement scale, relative error).

4. Results and discussions

4.1. Instrumented force-displacement curves

The force-displacement curves for specimens with their individual thickness and different strength & toughness are shown in Fig. 1. Except for the location and size of curves due to the initial ligaments of specimens that experience the different plastic bending work hardening before crack onset and the total impact energy absorbed, all the curves have the similar features as followed.

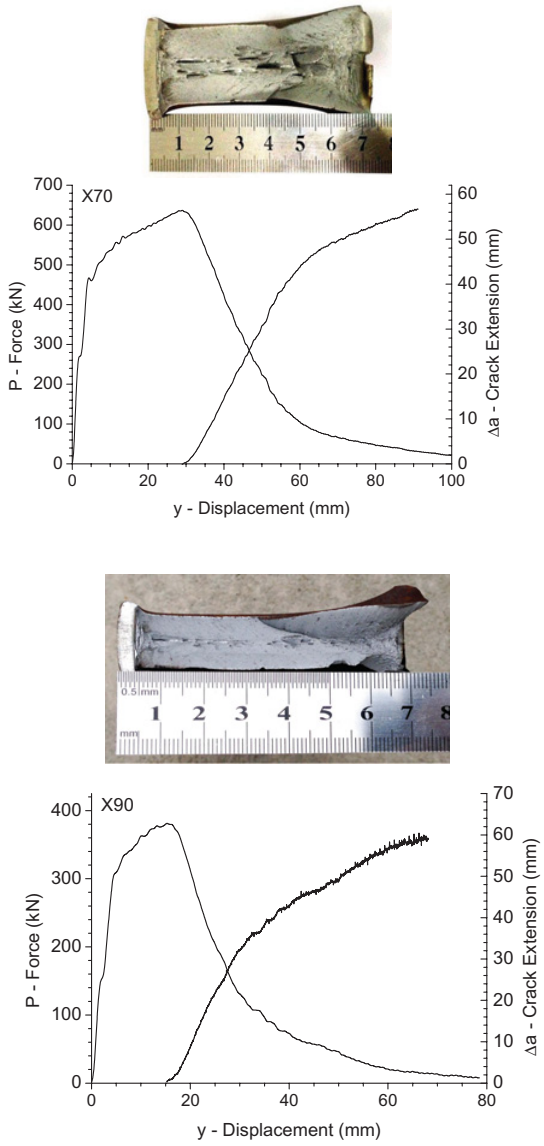

Figure 2. Dynamic crack extension Δa-y, from instrumented force-displacement relation by KC method, and its validation by measuring the region of stable cracking on the fracture surface.

It is clearly shown that after the initial elastic response, there is a significant plastic deformation before crack initiation. For convenience, here in the paper, the point at the maximum force is identified as the crack initiation nominally. Somewhere after the peak on the curve, the force starts to drop approximately linear with increasing tup displacement. Following the linear force-dropping period, the curve begins to tail off, due to the formation of shear lips, as shown in Fig. 2.

In some other works [7], the linear segment on the post-peak force-displacement curve was defined as the region of stable cracking. However $CTOA_C$ calculated within the range on the directly obtained force-displacement curve without any information or check about the real crack extension will confront the unforeseeable measurement deviation. For example, the influence of the initial cleavage zone nearby the notch root.

Table 1. The results of ($A^*\sigma_f$) from three typical high strength pipeline steel plates, and verification of the constant A^*.

No.	B mm	YS MPa	TS MPA	($A^*\sigma_f$) GPa	σ_f MPa	A^*
X70	31	506	641	0.261	746	0.35
X80	21	610	710	0.292	858	0.34
X90	16.9	680	800	0.293	962	0.30

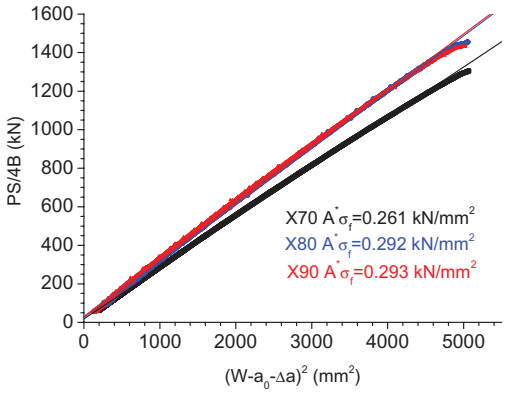

Figure 3. Plot of (PS/4B) vs. $[(W - a_0 - \Delta a)^2]$ relations for determining ($A^*\sigma_f$) as slope of linear regression.

4.2. Dynamic crack extension and constant of A*

Key-curve method deduced from the force-displacement curve of DWTT testing provides a way to study the entire cracking history, which is also recorded by the fracture surface. The calculated dynamic crack extension, e.g. the $\Delta a - y$, could be validated and confirmed by the direct measurement on the fracture surface, illustrated by Fig. 2.

Clearly on the fracture surface, the stable propagation featured by the region of silky and dull grey in appearance could be identified out of the initial cleavage fracture in bright-white & crystallite triangle area nearby the notch root, and the final formation of shear lips. As a result, the stable cracking of sample X70 is obtained nearly between the crack lengths of $10 \sim 40$ mm, and for sample X80 and X90, the regions are shortened to $10 \sim 35$ mm, in coincidence with the length of the linear segments indicated on the dynamic crack extension curve $\Delta a - v$.

In some works [3,6], the crack extension was estimated by limit loading hypothesis based on the change of the force over the propagation, compared with the maximum force at crack initiation, as Eq. (4).

$$P = \frac{4A^*\sigma_f B(W-a)^2}{S}. \tag{4}$$

Where, A^* is a material related constant (assumed to be 1/3 [8]), σ_f is a dynamic flow stress accurately determined from a high strain rate tensile. B is the thickness. $(W - a)$ is the remaining ligament. Derived from the limit loading hypothesis, a nearly linear correlation between (PS/4B) and $(W - a)^2$ might exist over the ductile fracture, which also offers an experimental way to obtain the parameter product of ($A^*\sigma_f$) that is required by some $CTOA_C$ algorithms [4].

In Table 1, the material based parameter product ($A^*\sigma_f$) was obtained as the slope of linear regression (PS/4B) vs. $(W\text{-}a_0\text{-}\Delta a)^2$ over the crack propagation, in Fig. 3. Here, dynamic crack extension Δa, was estimated by using KC method independently as above.

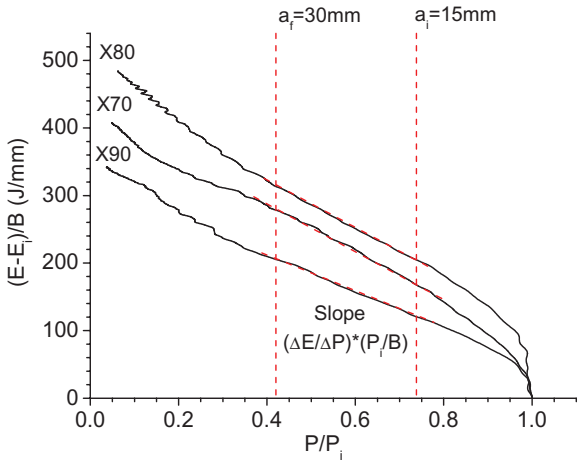

Figure 4. Plots of $[(E - E_i)/B]$ vs. (P/P_i) relations and linear regression for $CTOA_C$ as slope.

From Fig. 3, values of ($A^*\sigma_f$) for three typical high strength and toughness pipeline steels are 0.261 GPa for X70, 0.292 GPa for X80 and 0.293 GPa for X90 respectively. Moreover, once given the material properties, σ_f could be approximately evaluated as 1.3 times the average of yield and ultimate tensile strengths practically [6,9]. Therefore the unknown geometrical constant A* for these three steels were experimentally calculated about 0.30–0.35, verified very close to the commonly cited constant 1/3.

4.3. Estimation of $CTOA_C$

Towards the single-specimen energy based regression method, CTOAC could be determined with the input of regression slope ($\Delta E/\Delta P$) over the steady-state stage. The influence of specimen thickness was removed by normalizing Eq. (1) to obtain an equivalent expression shown as Eq. (5), for a convenient comparison of three sample all together.

$$CTOA_C = 2\arctan\left[\frac{-4Br^*}{P_i S}\cdot\frac{\Delta[(E-E_i)/B]}{\Delta(P/P_i)}\right]_{a_i \to a_f}. \tag{5}$$

The regression range in Eq. (5) is defined as the crack propagation from a_i to a_f, strictly confined in the region of stead-state stage that could be easily indicated from $\Delta a - y$ curve as introduced above. In the present paper, same regression range between $a_i = 15$ mm and $a_f = 30$ mm are selected for all three sample for a clear comparison, as shown in Fig. 4.

In the figure, from the right to left along the curve, energy is consumed for crack propagation with the load decreasing to zero. After crack initiation (i.e. maximum load point, $P/P_i = 1$), the slope of the curve is approximately constant in the portion illustrated by parallel vertical dashed lines, indicating the crack propagation from a_i to a_f.

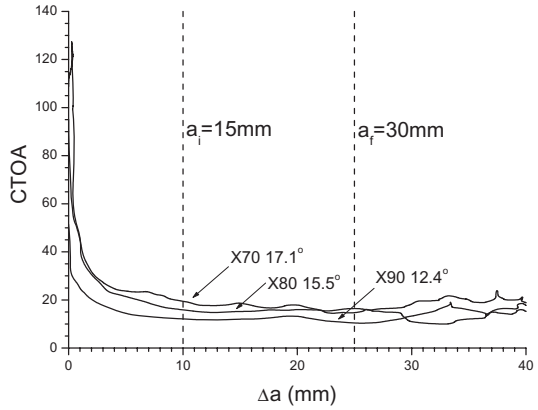

Figure 5. Plots of CTOA evolution for samples X70, X80 and X90 during crack propagation, indicating the stability of $CTOA_C$ over steady-state stage from a_i to a_f.

The x-axis of Fig. 4 is the inverse of crack extension and the slope of tangent at any point on the curve is related to the instantaneous CTOA value by Eq. (5).

(1) All samples show a similar evolution of CTOA value from crack initiation to thoroughly fracture, that is, the specimen experiences an high CTOA level, relative to the large slope of the curve, then followed by a constant $CTOA_C$ over the steady-state stage, and ends up with a rising period of CTOA due to shear lips, as shown in Fig. 5. This phenomenon has also been observed in other works by using in-situ high-speed video measurement for DWTT dynamically [9] and compact tension under quasi-static loading [10].

(2) Over the period of stable cracking, $CTOA_C$ is proportional to the absolute value of fitted slope. Samples X70 and X80 have the close values of $CTOA_C$ about 17.1° and 15.5° respectively, considerably higher than that of X90 about 12.4°. Similar values of CTOAC were also reported by Xu [11] in his study on the typical high grade pipeline steels X52-X100.

5. Conclusions

(1) Force-displacement curves of the standard V-notch pressed specimens sampled from three typical high grade X70, X80 and X90 pipeline steels were obtained by a 40kJ instrumented pendulum DWTT machine.

(2) Key-curve method was applied to evaluate the dynamic crack extension, Δa-y, helpful to define the region of stable ductile cracking that was also confirmed on the fracture surface. In the meanwhile, the validation of limit loading hypothesis was ascertained by linear fitting (PS/4B) vs. $(W - a_0 - \Delta a)^2$ relation, also providing an experimental way to the values of $(A^*\sigma_f)$. The value of A^* was acquired about 0.30–0.35, close to the commonly cited constant 1/3.

(3) The values of $CTOA_C$ indicates that X70 and X80 have nearly the same resistance to ductile fracture, higher than that of X90.

References

[1] D.J. Horsley, Engng. Fract. Mech. **70**, 547–552 (2003)
[2] J. Fang, J.W. Zhang, L. Wang, Int. J. Fract. **187**, 123–131 (2014)
[3] A. Martinelli, S. Venzi, Engng. Fract. Mech. **53**, 263–277 (1996)
[4] M. Di Biagio, A. Fonzo, G. Mannucci, et al. *Ductile fracture propagation resistance for advanced pipeline design* (GRI Report No. GRI-04/0129, Gas Research Institute, 2005)
[5] T. Kobayashi, I. Yamamoto, M. Niinomi, Engng. Fract. Mech. **24**, 773–782 (1986)
[6] S. Xu, R. Bouchard, W.R. Tyson, Engng. Fract. Mech. **74**, 2459–2464 (2007)
[7] G.M. Wilkowski, D.L. Rudland, Y.Y. Wang, D. Horsley, et al., *Proc. 4th International Pipeline Conference (IPC 2002)*, Paper IPC 2002–27132 (2002)
[8] J.F. Knott, *Fundamentals of Fracture Mechanics*, (Butterworths, London, 1973)
[9] D.L. Rudland, G.M. Wilkowski, Z. Feng, et al., Engng. Fract. Mech. **70**, 567–577 (2003)
[10] J.Q. Wang, J. Shuai, Engng. Fract. Mech. **79**, 36–49 (2012)
[11] S. Xu, W.R. Tyson, *Proc. 7th International Pipeline Conference (IPC 2008)*, Paper IPC 2008–64060 (2008)